DALTON

Metal complexes of a 12-membered tetraaza macrocycle containing pyridine and *N*-carboxymethyl groups*

Rita Delgado,[a,b] Sandra Quintino,[a] Miguel Teixeira[a,c] and Anjiang Zhang[a]

[a] *Instituto de Tecnologia Química e Biológica, Rua da Quinta Grande, 6, 2780 Oeiras, Portugal*
[b] *Instituto Superior Técnico, 1096 Lisboa codex, Portugal*
[c] *Universidade Nova de Lisboa, Faculdade de Ciências e Tecnologia, Monte da Caparica, Portugal*

The protonation constants of the macrocycle H_3L^1 [3,6,9,15-tetraazabicyclo[9.3.1]pentadeca-1(15),11,13-triene-3,6,9-triacetic acid] and the stability constants of its complexes formed with Mg^{2+}, Ca^{2+}, Mn^{2+}, Co^{2+}, Ni^{2+}, Cu^{2+}, Zn^{2+}, Cd^{2+}, Pb^{2+}, Ga^{3+}, Fe^{3+} and In^{3+} were determined by potentiometric methods, at 25 °C and ionic strength 0.10 mol dm^{-3} in tetramethylammonium nitrate. This macrocycle is not a selective ligand for the first-row transition divalent metal ions, exhibiting similar stability constants for all of them. The Irving–Williams order of stability is not obeyed, the complexes of Co^{2+} and Zn^{2+} having higher stability constants than those of Cu^{2+} and Ni^{2+}. The stability constants of alkaline-earth-metal ion complexes decrease with increasing ionic radius of the metal; however, those of Mg^{2+} and Ca^{2+} are of the same order. The stability of the iron(III) complex is lower than expected (log K_{ML} = 21.77). Based on spectroscopic measurements in solution (electronic and EPR) and the magnetic moments of the complexes, some explanations of the peculiarities of the formation of these complexes are proposed. The low value of the stability constant for the nickel(II) compared to that of the cobalt(II) complex is explained by the five-co-ordinate geometry adopted in each case. To explain the low stability of the copper(II) complex it is proposed that the ligand only co-ordinates *via* three of the four nitrogen donor atoms, the co-ordination being completed by two oxygen atoms of the acetate groups. The use of [FeL^1] as a model for iron proteins is proposed.

The search for new compounds which may form selective complexes with trivalent metal ions, such as Ga^{3+}, Fe^{3+} and In^{3+}, led us to study an *N*-acetate derivative of a pyridine-containing tetraazamacrocycle (H_3L^1), previously synthesized.[1] It is known that complexes formed by *N*-carboxymethyl derivatives of 12-membered macrocycles are very stable and that the stability decreases on increasing the number of atoms in the ring.[2–4] However, 12-membered ligands do not discriminate metal ions, the complexes with the first-row transition divalent metal ions exhibiting almost the same values of the stability constant.[2–4] In general, the Irving–Williams order of stability[5] is obeyed and no surprising inversions were observed.[2–4] For the alkaline-earth-metal ions, from Ca^{2+} to Ba^{2+}, the stability constants decrease regularly with increase in size of the macrocycle, no metal ion being particularly favoured. Although no surprising inversion of the usual trends of stability constants were observed, some remarkably stable complexes (thermodynamic and kinetically) were found, namely the 1,4,7,10-tetraazacyclododecane-1,4,7,10-tetraacetate (dota) complexes of Ca^{2+} [2] and of some trivalent lanthanides.[6–8] The thermodynamic and kinetic stability of the dota complexes with some trivalent metal ions make this ligand, in the form of its gadolinium complex, one of the most effective and safest contrast agents for magnetic resonance imaging (MRI) and it is also used in nuclear medicine, radioimmunoimaging or radioimmunotherapy. In the last cases, the dota complex of an appropriate radioisotope is usually covalently linked to a monoclonal antibody.[9] Many other derivatives of dota were synthesized and tested for those applications.[9] Although some progress was made, the major drawback to the use of these compounds remains the slow kinetics of complex formation,[10] an important limitation especially for radiopharmaceuticals.

The search for compounds which could have faster formation kinetics led us to the synthesis of H_3L^1. A study of a series

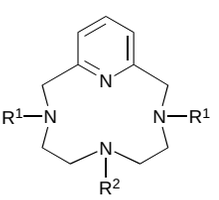

H_3L^1 R^1, R^2 = CH_2CO_2H
H_2L^2 R^1 = CH_2CO_2H, R^2 = H
L^3 R^1, R^2 = H

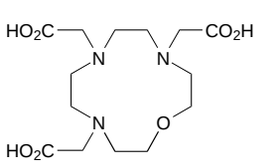

H_3L^4

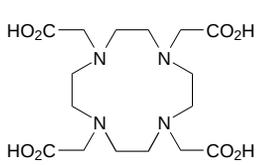

H_4dota

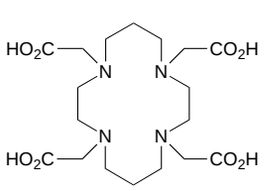

H_4teta

of cyclic tetraamines incorporating a pyridine has shown[11] not only that these compounds form complexes faster, but also that they have lower stability constants than those of the corresponding tetraaza macrocycles. The first observation was important enough to lead us to carry out the determination of the stability constants of H_3L^1 with a variety of di- and tri-valent metal ions. Although some years ago Stetter *et al.*[1] carried out a similar task for some divalent metal ions, our values are

* *Non-SI units employed:* $\mu_B \approx 9.27 \times 10^{-24}$ J T^{-1}, G = 10^{-4} T.

systematically higher than theirs. As stability constants are the first data to take into account in the selection of compounds for medical applications, because the complexes must have a sufficiently high stability to avoid competition with strong biological ligands, such as transferrin or ferritin, we decided to repeat the determinations, to extend the work to other metal ions, and to perform some spectroscopic measurements to understand the structure of some of the complexes in aqueous solution. Also, the overall basicity of H_3L^1 should be lower as pyridyl nitrogen is more acidic than tertiary amine nitrogen, so the competition of the ligand for the metal ion and for protons should be reduced at physiological pH. Recently, Sherry and co-workers[12] have synthesized a 12-membered compound containing pyridine in the ring and having two acetate groups, H_2L^2 and a similar one having two opposite pyridyl nitrogens, but few thermodynamic data were published. In another study they[13] performed relaxometry and luminescence measurements and animal biodistribution studies of some lanthanide(III) complexes with some ligands, among them H_3L^1.

The completely deprotonated forms of the macrocycles are $(L^1)^{3-}$ and $(L^2)^{2-}$ but for simplicity the charges will generally be omitted in the text.

Experimental

Reagents

The parent L^3 was synthesized and purified in our laboratory by previously reported procedures.[11] Chloroacetic acid and Dowex 1 × 8 ion-exchange resin (20–50 mesh) in the Cl^- form were obtained from BDH, triethylenetetramine tetrahydrochloride (trien·4HCl) from Aldrich-Chemie (97%) and K_2H_2edta (edta = ethylenedinitrilotetraacetate) from Fluka. All the chemicals were of reagent grade and used as supplied without further purification. The resin was treated with 1.0 mol dm^{-3} formic acid before use. The organic solvents were purified by standard methods.[14]

Synthesis and characterisation

The compound H_3L^1 was synthesized by condensation of the parent L^3 (1.114 mmol, 0.5 g) with potassium chloroacetate (obtained by addition of 3 mol dm^{-3} KOH solution to concentrated aqueous chloroacetic acid, 3.70 mmol, 0.35 g, at 5 °C) in aqueous basic solution (≈ 1 cm^3). The temperature was increased slowly during the reaction to a maximum of 75 °C and the pH was kept below 10, by slow addition of 3 mol dm^{-3} KOH. In 90 h the reaction had reached completion; then the mixture was cooled and adjusted to pH 2.0 with 5 mol dm^{-3} hydrochloric acid. Upon removal of solvent *in vacuo* a small amount of methanol was added. The inorganic matter formed was filtered off and the filtrate with the desired product purified by chromatography using an anionic resin in the formate form (column 22.0 × 2.0 cm). The flow rate was kept at 1.0 cm^3 min^{-1}. After washing with water (250 cm^3), the final product was eluted with a solution of 0.02 mol dm^{-3} formic acid (500 cm^3). The pure product was isolated as a white solid upon concentration and chilling of the solution. Yield: 49%. M.p. 226–228 °C (decomp.). NMR (D_2O, pD 3.8): ^{1}H [sodium 4,4-dimethyl-4-silapentane-1-sulfonate (dss) as reference], δ 7.98 (1 H, t), 7.48 (2 H, d), 4.85 (4 H, s), 4.03 (4 H, s), 3.60 (2 H, s), 3.49 (4 H, t) and 3.01 (4 H, t), ^{13}C (1,4-dioxane), δ 174.66, 170.11, 150.40, 140.01, 122.56, 59.44, 57.96, 55.81, 54.01 and 51.38 (Found: C, 49.2; H, 6.5; N, 13.4. Calc. for $C_{17}H_{24}N_4O_6$·$2H_2O$: C, 49.05; H, 6.8; N, 13.45%).

Potentiometric measurements

Reagents and solutions. Metal-ion solutions were prepared at about 0.050 mol dm^{-3} from the nitrate salts of the metals, of analytical grade, with demineralised water (obtained by a Millipore/Milli-Q system) and were standardised by titration with K_2H_2edta. Solutions of the trivalent metal ions were kept in an excess of nitric acid to prevent hydrolysis. Carbonate-free solutions of the titrant, NMe_4OH, were prepared as described.[4] Solutions were discarded when the percentage of carbonate was about 0.5% of the total amount of base.

Equipment and working conditions. The equipment used was as described.[15] All the experiments were monitored by computer. The temperature was kept at 25.0 ± 0.1 °C; atmospheric CO_2 was excluded from the cell by passing purified N_2 across the top of the experimental solution. The ionic strength of the solutions was kept at 0.10 mol dm^{-3} with NMe_4NO_3.

Measurements. The $[H^+]$ of the solutions was determined by the measurement of the electromotive force of the cell, $E = E'^\circ + Q \log [H^+] + E_j$; E'° and Q were obtained by previous calibration, titrating a standard solution of known hydrogen-ion concentration at the same ionic strength, using the values of the acid range. The term pH is defined as $-\log [H^+]$. the liquid-junction potential, $E_j = j_H[H^+] + j_{OH}[OH^-]$, where j_H and j_{OH} were determined by an acid–base titration of concentrated solutions,[16] was found to be negligible under the experimental conditions used. The value of $K_w = [H^+][OH^-]$ was determined from data obtained in the alkaline range of the calibration, considering E'° and Q valid for the entire pH range, and found equal to $10^{-13.80}$ mol^2 dm^{-6}.

The potentiometric equilibrium measurements were made on macrocycle solutions (≈2.50×10^{-3} mol dm^{-3}, 20.00 cm^3), diluted to a final volume of 30.00 cm^3, first in the absence of metal ions and then in the presence of each metal ion for which the $c_L : c_M$ ratios were 1:1, 1:2 and in several cases 2:1. The E data were taken after additions of 0.025 or 0.050 cm^3 increments of standard 0.109 mol dm^{-3} NMe_4OH solution, and after stabilisation in this direction equilibrium was then approached from the other direction by adding standard 0.105 mol dm^{-3} nitric acid solution.

In the cases of Cu^{2+}, Ga^{3+}, Fe^{3+} and In^{3+} ligand–ligand or metal–metal competition titrations were performed. Triethylenetetramine (L′) was used as the second ligand in the case of the copper complex, in the ratio of 1:1:1 ($c_{L^1} : c_{L'} : c_M$). The competition reaction can be written in terms of equilibrium (1)

$$[ML']^{2+} + [H_5L^1]^{2+} \rightleftharpoons [ML^1]^- + 3H^+ + [H_2L']^{2+} \quad (1)$$

(M = Cu^{2+}, L′ = trien), and was considered adequate when all complexed species existed in solution at least in a 30% concentration with respect to the total metal ions.

For the gallium complex the competition or displacement reaction (2)[15] which starts at pH ≈ 6 was used.

$$[GaL^1] + 4OH^- \rightleftharpoons [Ga(OH)_4]^- + (L^1)^{3-} \quad (2)$$

It was impossible to find an adequate second ligand for the competition with the iron(III) complex of L^1; K_2H_2edta was tried but unsuccessfully, so a direct redox titration was used. In this case the Fe^{2+}–Fe^{3+} system, in excess of Fe^{2+}, was monitored by platinum and reference electrodes, by addition of the macrocycle, at pH 2.[17] For the indium(III) complex the same experimental method was used, following the competition reaction between Fe^{3+} and In^{3+} for the macrocycle.[17]

As the stability constant for the copper complex of L^1 obtained was lower than expected two other techniques were used: (1) a competition titration with another metal ion, Fe^{3+} being the second metal ion chosen, in the ratio 2:1:1, $c_{L^1} : c_M : c_{M'}$ and (2) a direct spectroscopic titration, in the range pH 2.24–7.05, 1:1 M:L^1 ratio, the initial concentration of the

metal ion being 1.551×10^{-3} mol dm^{-3} and in the visible region, 900–600 nm.

In the competing reactions the equilibria were slow to attain but automated titrations were possible, though it was necessary to wait about 10–15 min at each point of the titration in the pH range where competition took place. The same values of the stability constants were obtained either by using the direct or the back titration curves. The metal–metal competition reactions, using the redox titration, were slower to equilibrate; 20–30 min were, in general, necessary.

Calculation of equilibrium constants. Protonation constants $K_i^{\mathbf{H}} = [H_iL]/[H_{i-1}L][H]$ were calculated by fitting the potentiometric data obtained for the free macrocycle using the SUPERQUAD program.[18] Stability constants of the various species formed in solution were obtained from the experimental data corresponding to the titration of solutions of different ratios of the ligand and metal ions, also with the aid of the SUPERQUAD program. The results were obtained in the form of overall stability constants or $\beta_{\mathbf{M}_m\mathbf{H}_h\mathbf{L}_l} = [M_mH_hL_l]/[M]^m[L]^l[H]^h$.

Only mononuclear species, ML, M(HL) and MLH_{-1} ($\beta_{\mathbf{MLH}_{-1}} = \beta_{\mathbf{ML(OH)}}K_{\mathbf{W}}$) were found. Differences, in log units, between the values of $\beta_{\mathbf{M(HL)}}$ (or $\beta_{\mathbf{MLH}_{-1}}$) and $\beta_{\mathbf{ML}}$ provide the stepwise protonation reaction constants. The errors quoted are the standard deviations of the overall stability constants given directly by the program. In the case of the stepwise constants the standard deviations were determined by the normal propagation rules and do not represent the total experimental errors. Species distribution curves were plotted with the aid of the program SPE and SPEPLOT.[19] The protonation constants were obtained from 200 experimental points (four titration curves) and stability constants for each metal ion from 75 (for the alkaline-earth-metal ions) to 260 (for Cu^{2+}) experimental points (two to six titration curves). For the spectrophotometric titration the SQUAD program[20] was used.

Hydrolysis of trivalent metal ions. The trivalent metal ions studied easily form hydrolytic species in aqueous solution, the constants for which have some discrepancies in the literature. We used the values presented.[15,21]

Spectroscopic studies

Proton NMR spectra were recorded with a Bruker CXP-300 spectrometer. Solutions of the macrocycle (≈0.01 mol dm^{-3}) were made up in D_2O and the pD was adjusted by addition of DCl or CO_2-free KOD, using an Orion 420A instrument fitted with a combined Ingold microelectrode. The $-\log [D^+]$ was measured directly in the NMR tube, after calibration of the microelectrode with buffered aqueous solutions; dss was used as an internal reference. The ^{13}C NMR spectra were recorded with the same spectrometer and 1,4-dioxane as internal reference. The metal complexes were prepared in water by addition of the metal ion, in the form of nitrate salts, to an equivalent amount of the macrocycle and enough KOH to the final pH, and after evaporation of water were dissolved in D_2O. Magnetic moments of the complexes were determined by the Evans method in solution[22] at room temperature.

Electronic spectra were measured with a Shimadzu model UV-3100 spectrophotometer for UV/VIS/near IR, using aqueous solutions of the complexes prepared as indicated above.

The X-band EPR spectra were recorded with a Bruker ESP 380 spectrometer equipped with a continuous-flow cryostat for liquid helium or for liquid nitrogen. The spectra of the complexes of Cu^{2+} and Fe^{3+} (1.55×10^{-3} and 1.68×10^{-3} mol dm^{-3} respectively, in 1.0 mol dm^{-3} $NaClO_4$) were recorded at 100.0 K for the first complex, 4.6, 100.0 and 200.0 K for the second. The EPR spectrum of the copper complex was simulated with a program for a microcomputer.[23]

Table 1 Protonation (log $K_i^{\mathbf{H}}$) constants of L^1–L^4 and dota (25.0 °C, $I = 0.10$ mol dm^{-3})

Equilibrium quotient	log $K_i^{\mathbf{H}}$				
	L^1	L^{2a}	L^{3b}	L^{4c}	dota[d]
[HL]/[H][L]	10.90(1); 10.6[e]	12.5	10.33	11.61	12.09
$[H_2L]/[HL][H]$	7.11(1); 7.6[e]	5.75	7.83	7.70	9.76
$[H_3L]/[H_2L][H]$	3.88(2); 4.4[e]	3.28	(1.27)	4.05	4.56
$[H_4L]/[H_3L][H]$	2.27(3)	2.38	<1	2.77	4.09
$[H_4L]/[L][H]^4$	24.16	23.9	<20.43	26.13	30.50

[a] $I = 0.1$ mol dm^{-3} KCl, ref. 12. [b] $I = 0.10$ mol dm^{-3} KNO_3, ref. 11. [c] $I = 0.10$ mol dm^{-3} NMe_4NO_3, ref. 24. [d] $I = 0.10$ mol dm^{-3} NMe_4NO_3, refs. 2 and 3. [e] $I = 0.1$ mol dm^{-3} KCl 20 °C, ref. 1.

Results

Protonation and stability constants

For the solution equilibrium studies $[H_4L^1][NO_3]$ was prepared by adding 1 equivalent of HNO_3 to H_3L^1. In this form, the macrocycle gave a titration curve with two inflection points, at $a = 2$ and 3, respectively (a being the number of equivalents of base added per mol of macrocycle). The protonation constants obtained for L^1 are summarised in Table 1 together with the values of some other tetraaza and one oxatriaza macrocycles for comparison.

The titration curves obtained for mixtures of the macrocycle L^1 and metal ions (1:1) showed one inflection at $a = 4$, with the exception of those corresponding to Ga^{3+}, Fe^{3+} and In^{3+}. In those cases the curves present a strange inflection at $a = 4.5$ owing to the formation of stable hydroxo species at low pH. As precipitation occurs immediately after the inflection, our first model for calculation of the stability constants involved an ML(OH) species, in the supposition that the premature precipitation of the hydroxo complex would lead to a steep increase in the pH. This model was not accepted by SUPERQUAD. However, it did accept the $M_2L_2(OH)^-$ species, in which one hydroxide links two ML complexes, which is not neutral and will probably rearrange to form M_2L_2O. Titration curves of the complexes of Mg^{2+}, Ca^{2+} and Ba^{2+} exhibit another inflection at $a = 2$, where the formation of complexes starts. Titration curves corresponding to other mixtures, *e.g.* in 2:1 or 1:2 ratio do not present significant differences from those of ratio 1:1.

The values of the stability constants for the metal complexes of L^1 studied in this work (Mg^{2+}, Ca^{2+} and Ba^{2+}, first-row transition-metal ions, Cd^{2+} and Pb^{2+} and some trivalent metal ions, Ga^{3+}, Fe^{3+} and In^{3+}), determined in water, are compiled in Table 2. In most cases only ML and M(HL) species are formed, but hydroxo complexes ML(OH) are also found for many divalent first-row transition-metal ions. For the complexes of Ga^{3+}, Fe^{3+} and In^{3+}, as discussed, an $M_2L_2(OH)^-$ species seems to be formed, which precipitates at pH values of about 4.3 for Fe^{3+} and 4.9 for In^{3+}; however, in the case of Ga^{3+} the precipitation does not occur as the species dissociates to form the stable ion $[Ga(OH)_4]^-$. We have checked the possibility of formation of other species like protonated, MH_iL ($i \geqslant 2$), or polynuclear M_2L, but they do not appear to be formed under our conditions.

As the overall basicity of L^1 is not very high the complexes of Fe^{3+} and In^{3+} were completely or almost completely formed at low pH, therefore the stability constants were determined by competition reactions or by a redox method. For Cu^{2+} the data were also checked by a competition reaction and a spectrophotometric method, as its constants are lower than expected. The values of the protonation and stability constants of trien and edta used as the second ligand were determined by us (*cf.* Table 3), but compare very well with the literature values.[26] Fig. 1 shows the species distribution diagram of the metal–metal competition reaction between L^1, Fe^{3+} and Cu^{2+} obtained with

Table 2 Stability constants (log $K_{\mathbf{M}_m\mathrm{H}_h\mathrm{L}_l}$) of some metal complexes L^1–L^4 and dota (25.0 °C, I = 0.10 mol dm^{-3})

Ion	Equilibrium quotient	log $K_{\mathbf{M}_m\mathrm{H}_h\mathrm{L}_l}$ L^1	L^2 [a]	L^3 [b]	L^4	dota
Mg^{2+}	[ML]/[M][L]	11.82(1); 7.2 [c]	8.4	—	10.254 [d]	11.92 [e]
	[M(HL)]/[ML][H]	3.70(6)	—	—	5.67 [d]	4.09 [e]
	[ML]/[ML(OH)][H]	—	—	—	—	—
Ca^{2+}	[ML]/[M][L]	12.379(6); 8.3 [c]	10.0	—	12.984 [d]	17.23 [e]
	[M(HL)]/[ML][H]	3.66(5)	—	—	3.93 [d]	3.54 [e]
Ba^{2+}	[ML]/[M][L]	9.131(6)	—	—	9.915 [d]	12.87 [e]
	[M(HL)]/[ML][H]	4.87(1)	—	—	6.04 [d]	5.63 [e]
Mn^{2+}	[ML]/[M][L]	18.59(1)	—	8.81	16.09 [d]	20.20 [f]
	[M(HL)]/[ML][H]	2.21(3)	—	—	4.14 [d]	4.15 [f]
	[ML]/[ML(OH)][H]	8.71(9)	—	—	—	—
Co^{2+}	[ML]/[M][L]	18.92(2); 13.3 [c]	—	(15.69)	19.54 [d]	20.27 [e]
	[M(HL)]/[ML][H]	2.95(4)	—	—	2.64 [d]	4.08 [e]
	[ML]/[ML(OH)][H]	9.45(5)	—	—	—	—
Ni^{2+}	[ML][M][L]	17.31(2)	—	17.05	18.04 [d]	20.03 [e]
	[M(HL)]/[ML][H]	3.91(3)	—	—	3.66 [d]	3.51 [e]
	[ML]/[ML(OH)][H]	9.8(1)	—	—	—	—
Cu^{2+}	[ML]/[M][L]	17.49(4); 14.3 [c]	—	20.14	20.17 [d]	22.25 [e]
	[M(HL)]/[ML][H]	4.03(4)	—	—	3.10 [d]	3.78 [e]
	[ML]/[ML(OH)][H]	10.3(1)	—	7.48	—	—
Zn^{2+}	[ML]/[M][L]	18.22(3); 13.3 [c]	—	14.40	18.66 [d]	21.099 [f]
	[M(HL)]/[ML][H]	3.64(4)	—	—	2.85 [d]	4.178 [f]
	[ML]/[ML(OH)][H]	9.4(1)	—	8.5	—	—
Cd^{2+}	[ML]/[M][L]	19.53(6); 13.8 [c]	—	12.670	19.25 [g]	21.31 [f]
	[M(HL)]/[ML][H]	2.5(1)	—	—	—	4.39 [f]
	[ML]/[ML(OH)][H]	—	—	10.44	—	—
Pb^{2+}	[ML]/[M][L]	17.48(1); 13.7 [c]	—	15.422	19.18 [g]	22.69 [f]
	[M(HL)]/[ML][H]	3.78(1)	—	—	—	3.86 [f]
	[ML]/[ML(OH)][H]	—	—	10.58	—	—
Ga^{3+}	[ML]/[M][L]	19.37(6)	—	—	21.3 [h]	21.33 [i]
	[M(HL)]/[ML][H]	2.7(1)	—	—	2.66 [h]	4.00 [i]
	[ML]/[ML(OH)][H]	—	—	—	7.84 [h]	—
	$[ML]^2/[M_2L_2(OH)][H]$	3.2(1)	—	—	—	—
Fe^{3+}	[ML]/[M][L]	21.77(5)	—	—	26.8 [h]	29.4 [i]
	[M(HL)]/[ML][H]	1.74(7)	—	—	2.17 [h]	3.23 [i]
	[ML]/[ML(OH)][H]	—	—	—	7.75 [h]	—
	$[ML]^2/[M_2L_2(OH)][H]$	1.8(1)	—	—	—	—
In^{3+}	[ML]/[M][L]	21.42(7)	—	—	25.48 [h]	23.9 [i]
	[M(HL)]/[ML][H]	1.8(1)	—	—	1.8 [h]	3.44 [i]
	[ML]/[ML(OH)][H]	—	—	—	9.59 [h]	—
	$[ML]^2/[M_2L_2(OH)][H]$	2.1(1)	—	—	—	—

[a] I = 0.1 mol dm^{-3} KCl, ref. 12. [b] I = 0.10 mol dm^{-3} KNO_3, ref. 11. [c] I = 0.1 mol dm^{-3} KCl, 20 °C, ref. 1. [d] I = 0.10 mol dm^{-3} NMe_4NO_3, ref. 24(*a*). [e] I = 0.10 mol dm^{-3} NMe_4NO_3, ref. 2. [f] I = 0.10 mol dm^{-3} NMe_4NO_3, ref. 3. [g] I = 0.10 mol dm^{-3} NMe_4NO_3, ref. 24(*b*). [h] I = 0.10 mol dm^{-3} KCl, ref. 21. [i] I = 0.10 mol dm^{-3} KCl, ref. 25.

Table 3 Protonation (log $K_i^{\mathbf{H}}$) constants of edta and trien and their stability constants (log $K_{\mathbf{M}_m\mathrm{H}_h\mathrm{L}_l}$) with metal ions used in competition reactions (25.0 °C, I = 0.10 mol dm^{-3})

Ion	Equilibrium quotient	edta	trien
H^+	[HL]/[H][L]	10.22(2); [a] 10.19 [b]	9.62; [a] 9.74 [b]
	$[H_2L]/[HL][H]$	6.05(1); [a] 6.13 [b]	9.00; [a] 9.07 [b]
	$[H_3L]/[H_2L][H]$	2.71(2); [a] 2.69 [b]	6.51; [a] 6.59 [b]
	$[H_4L]/[H_3L][H]$	2.0(1); [a] 2.00 [b]	3.14; [a] 3.27 [b]
Cu^{2+}	[ML]/[M][L]	—	20.24(2); [a] 20.05 [b]
	[M(HL)]/[ML][H]	—	3.55(2); [a] 3.70 [b]
	[ML]/[ML(OH)][H]	—	9.2(1); [a] 9.35 [b]
Fe^{3+}	[ML]/[M][L]	24.95(4); [a] 25.10 [b]	—
	[M(HL)]/[ML][H]	—; [a] 1.3 [b]	—
	[ML]/[ML(OH)][H]	7.41(3); [a] 7.37 [b]	—

[a] This work, I = 0.10 mol dm^{-3} NMe_4NO_3. [b] Ref. 26(*a*).

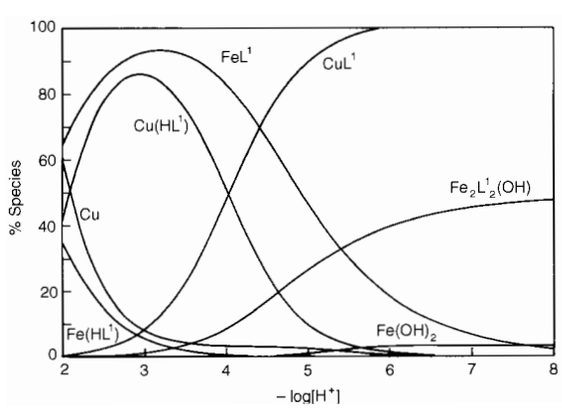

Fig. 1 Species distribution curves calculated for an aqueous solution containing L^1, Cu^{2+} and Fe^{3+} at a molar ratio of 2:1:1. The concentrations are relative to the total amount of Cu^{2+} at an initial value of 8.467 × 10^{-4} mol dm^{-3}

the SPE program [19] and Fig. 2 the species distribution diagram of the gallium complexes, showing the pH region of stability of $M_2L_2(OH)^-$ and its decomposition to $[Ga(OH)_4]^-$.

Spectroscopic studies

The UV/VIS/near-IR data for complexes of Co^{2+}, Ni^{2+}, Cu^{2+} and Fe^{3+} with L^1 in water are collected in Table 4. The electronic spectrum of the cobalt complex exhibits four broad bands at 1160, 823, 513 and 295.7 nm (ε = 2.3, 5.3, 33.1 and 795.0 dm^3 mol^{-1} cm^{-1}, respectively) and some other small bands in the near-IR region. The magnetic moment is 4.34 μ_B. This pink complex is slow to form (4.5 h were needed to reach the maximum absorbance of a 1:1 mixture of the metal ion and the macrocycle at pH 6.4), but did not suffer degradation with time,

Table 4 The UV/VIS/near-IR data and magnetic moments for the complexes of Co^{2+}, Ni^{2+}, Cu^{2+} and Fe^{3+} with L^1 (25.0 °C)

Complex	pH, colour	λ_{max}/nm (ε/dm^3 mol^{-1} cm^{-1})	μ/μ_B
$[CoL^1]^-$	6.4, pink	1160 (2.3), 1125 (1.9), 823 (5.3), 513 (33.1), 486.2 (sh) (30.4), 295.7 (795.0)	4.34
$[NiL^1]^-$	7.71, violet	1166 (sh) (11.9), 954.3 (36.0), 628.2 (sh) (5.1), 547.7 (12.7), 335.7 (98.1), 290 (235.4)	3.25
$[CuL^1]^-$	6.08, turquoise	1260 (18.7), 770 (sh) (80.0), 720 (104.6), 299 (2200), 263 (5300)	1.8
$[FeL^1]$	3.47, yellow	440 (sh) (26), 286.8 (16 000), 257.9 (24 000)	5.55

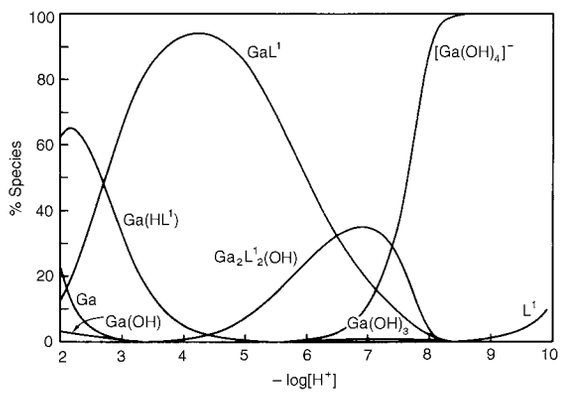

Fig. 2 Species distribution curves calculated for an aqueous solution containing L^1 and Ga^{3+} at a molar ratio of 1:1. Percentages relative to the total amount of Ga^{3+} at an initial value of 1.650×10^{-3} mol dm^{-3}

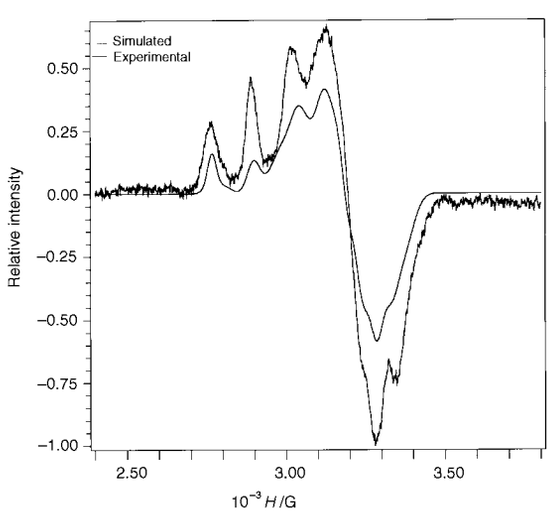

Fig. 3 The X-band EPR spectrum of the copper complex of L^1 in 1.0 mol dm^{-3} $NaClO_4$ recorded at 100.0 K, ν = 9.41 GHz, microwave power 2.4 mW and modulation amplitude 1 mT, and its simulated spectrum taking into account both isomers

at room temperature, although a fast oxidation occurred when the solution was concentrated at 60 °C under vacuum. The violet solution of the nickel complex exhibits four main bands at 954.3, 547.7, 335.7 and 290 nm (ε = 36.0, 12.7, 98.1 and 235.4 dm^3 mol^{-1} cm^{-1}, respectively) and a magnetic moment of 3.25 μ_B. The copper complex is turquoise exhibiting a broad band in

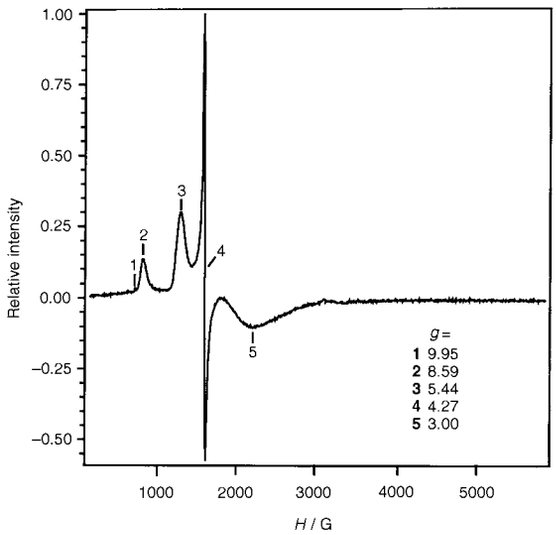

Fig. 4 The X-band EPR spectrum of the iron complex of L^1 in 1.0 mol dm^{-3} $NaClO_4$ recorded at 4.6 K, ν = 9.64 GHz, microwave power 2.4 mW and modulation amplitude 1 mT

the visible region at 720 nm with a shoulder at lower energies (770 nm), due to the copper d–d transitions, one small band in the near-IR region and two intense bands in the ultraviolet region, at 299 and 263 nm. The spectrum of the yellow iron complex shows two intense peaks at 286.8 and 257.9 nm and a large band in the visible at 440 nm with a shoulder at higher energies. The magnetic moment is 5.55 μ_B.

The EPR spectra of the complexes of Cu^{2+} and Fe^{3+} are shown in Figs. 3 and 4. The spectrum of $[CuL^1]^-$ exhibits three well resolved lines of the four expected at low field due to the interaction of the unpaired electron spin with the copper nucleus, and no superhyperfine splitting due to coupling with the four nitrogen atoms of the macrocycle. The fourth copper line is completely overlapped by the much stronger and unresolved band of the high-field part of the spectrum. The computational simulation of the spectrum[23] was only possible when a mixture of two copper species was considered, each having three different principal g values, indicating that the Cu^{2+} ions in these complexes are both in a rhombically distorted ligand field. The $[FeL^1]$ EPR spectra obtained are typical of rhombic iron(III) complexes in the high-spin state, in agreement with the determined magnetic moment. The dominant resonances are observed at g values 9.95, 8.59, 5.44, 4.27 and a broad signal in the region of about 3, the relative intensities of which do not change in the temperature range used.

Discussion

The macrocycle L^1 has seven basic centres, but only four protonation constants were obtained; the last three are too low to be determined by potentiometric measurements. All the compounds listed in Table 1 have two high (or fairly high) and two low values of the protonation constants. The first two are similar to those of the corresponding parent L^3, and due to the protonation of two nitrogen atoms of the ring in opposed positions, minimising electrostatic repulsions. The last two, certainly corresponding to protonation of carboxylate groups of L^1, differ from that of L^3 which involves protonation of the last two amines of the macrocycle. Of interest is the low value of the second protonation constant of L^1, even lower than that of the corresponding value of L^3. As shown by a ^{1}H NMR titration for L^3,[11] the low value of K_2 is due to the protonation of the pyridyl nitrogen and probably the same occurs with L^1. Particularly intriguing is the very high K_1 and the low K_2 value found for L^2,[12] for which we do not have an explanation. It is true that the log protonation constant of a pyridyl nitrogen in a

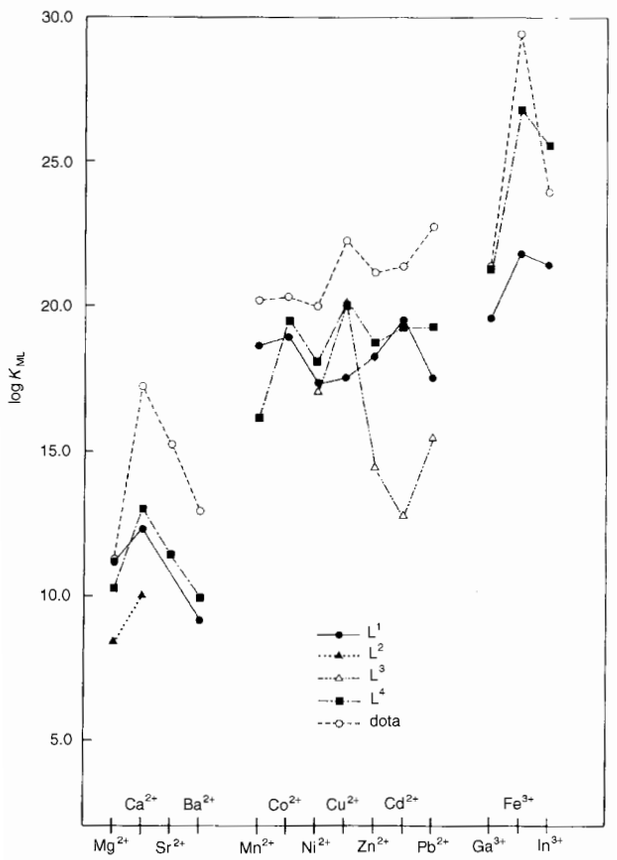

Fig. 5 Variation of the stability constants (log K_{ML}) of the metal complexes of L^1 and other similar macrocycles with the atomic number of the metal ion

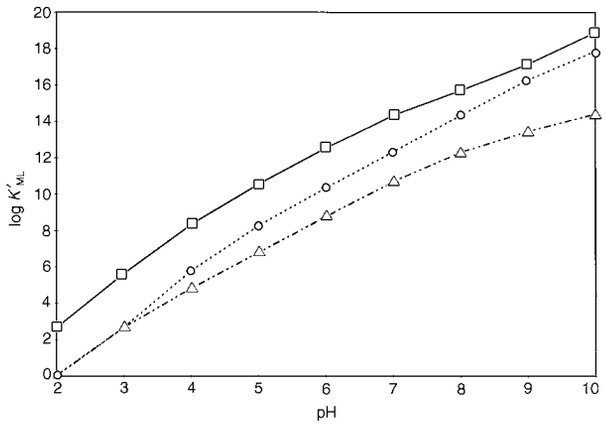

Fig. 6 Variation of the conditional stability constants (log K'_{ML}) of the manganese(II) complexes of L^1 (□), dota (◇) and L^4 (△)

linear compound has, in general, a value of about 5.8. However, protonation constants of the first two nitrogens of a macrocycle of small cavity (12- to 14-membered ring) are generally higher than those of linear compounds and the usual explanation for this is the possible stabilisation of the protonated species by hydrogen bonds. In the case of L^1 the proton bound to the pyridyl nitrogen, after protonation, should be stabilised by hydrogen bonds with the two adjacent nitrogen atoms. The third protonation constant has a normal value for a carboxylate linked to a non-protonated amine favouring the formation of intramolecular hydrogen bonds between non-protonated nitrogen and protonated carboxylate groups,[27,28] probably spreading over the two carboxylates bound to the amines adjacent to the pyridyl. The fourth protonation constant has a very low value, explained only if it corresponds to a carboxylate bound to a nitrogen amine already protonated,[27,28] that is to the carboxylate linked to the ammonium group opposed to the pyridine. The lower values of the second and fourth constants of L^1 contribute strongly to a lower overall basicity compared to that of dota (a decrease of more than 6 log units), a fact with strong repercussions in the metal complexation of L^1.

There are some differences between the protonation constants published by Stetter *et al.*[1] and ours (*cf.* Table 1). The higher value of K_1 obtained in the present work certainly arises from our use of a non-complexing medium, namely tetramethylammonium nitrate, while the previous authors used KCl. However, the differences are larger for the last two constants and for that we have no explanation. Also, the values of the stability constants of the complexes determined in this work, Table 2, are significantly different from those obtained by Stetter *et al.*[1] for all the metal ions for which those authors published values. In all cases the values previously published are smaller, differences for the ML species (the only one for which they have values) being between 3.19 and 5.73 log units. These large differences cannot be explained by differences in temperature or the ionic medium used, or even in the protonation constants.

Consideration of the stability constants in Table 2 and their variation in Fig. 5 allows some interesting conclusions. (1) Compound L^1 is not a selective ligand for the first-row transition divalent metal ions, resulting in similar stability constants for all of them, a behaviour which is shared by other *N*-carboxymethylated derivatives of 12-membered macrocycles, such as dota[2,3] and L^4,[24] as observed in Fig. 5. Specific to L^1 are the low stability constants of the complexes of Cu^{2+} and Ni^{2+}. The Irving–Williams order of stability is not obeyed, the complexes of Co^{2+} and Zn^{2+} having higher stability constants than those of Cu^{2+} and Ni^{2+}. Also, the lead complex has a lower stability constant than expected when compared with corresponding values of dota or L^4 complexes. (2) The alkaline-earth-metal ion complexes of L^1 exhibit a normal trend, the stability constants decreasing with increase in ionic radius of the metal. However, the value for the magnesium complex is of the same order as that of the calcium one and equal to that of the corresponding dota complex. (3) The trivalent metal ion complexes of L^1 exhibit the usual trend for polyaminopolycarboxylate complexes, that of iron showing the higher stability. Nevertheless the value for this complex is lower than expected by comparison with those of Ga^{3+} or In^{3+}, or with the dota complex. (4) In general, L^1 complexes have lower stability constants than those of the corresponding dota complexes, this being expected as dota has a higher overall basicity and one more acetate group for the co-ordination. However, it was shown that the dota when co-ordinated to the first-row transition-metal ions, forming complexes mainly by covalent interactions, does not use all its donor atoms. For the complexes of Cu^{2+} and Ni^{2+} this was observed both by spectroscopy in solution and X-ray diffraction analysis of crystals.[29–31] The ML complexes do not bind two acetate groups linked to opposite nitrogen atoms,[30] and these free acetate groups may be involved in bi- or poly-nuclear species,[29,31] So, the lower stability of L^1 complexes compared with those of dota is in most cases due to the lower overall basicity of L^1 (a difference of 6.34 log units[2,3]). However, in general, the stabilities of corresponding complexes of both ligands differ by a lower amount, in certain cases much lower, than the mentioned difference in basicities (the difference, in log units, being 0.1 for Mg^{2+}, 1.61 for Mn^{2+}, 1.35 for Co^{2+}, 2.72 for Ni^{2+}, 2.88 for Zn^{2+}, 1.78 for Cd^{2+}, 1.96 for Ga^{3+} and 2.48 for In^{3+}). This means that the competition between protons and metal ions for L^1 is lower than in the dota case, favouring the formation of complexes of L^1. For the complexes of those metal ions, L^1 is a better ligand than dota, over the entire pH scale, as illustrated in Fig. 6 for Mn^{2+}. The opposite was found for Ca^{2+}, Ba^{2+}, Cu^{2+}, Pb^{2+} and Fe^{3+}. Fig. 7 illustrates this situation for Cu^{2+}. These considerations account for the thermo-

Table 5 The pM[a] values for complexes of Ga^{3+} and In^{3+} with L^1 and dota at pH 7.4

	L^1	dota[b]
pGa	16.58	15.86
pIn	19.07	16.85

[a] Calculated for a 100% excess of free macrocycle under physiological conditions (pH 7.4, $c_M = 1.0 \times 10^{-5}$ mol dm^{-3}, $c_L = 2.0 \times 10^{-5}$ mol dm^{-3}) using the SPE program.[19] [b] Calculated from published stability constants.[2,25]

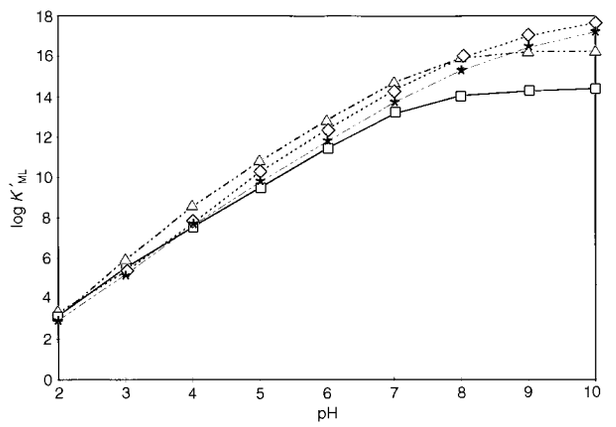

Fig. 7 Variation of the conditional stability constants (log K'_{ML}) of the copper(II) complexes of L^1 (□), dota (◇), teta (*) and L^4 (△)

dynamic behaviour of the complexes, but even without precise kinetics studies we have observed that complex formation is faster for L^1 than for dota. For instance, the nickel complexes which are the slowest to equilibrate takes on average 13 min at each point of the titration (at one point, 25 min) with L^1 and around 1 week with dota, the titration of which needed a batch method.[2,3] The cases where L^1 presents a better behaviour than dota, similar to that shown in Fig. 6, should be explained by a special structural arrangement of the ligand on complexation and/or by a different chemical interaction due to the presence of a pyridyl nitrogen in the skeleton of the macrocycle. The stability constants of metal complexes of linear ligands containing pyridyl donors tend to be higher than would be predicted on the basis of the protonation constants.[11,32] The enhanced stabilities of these complexes were partially attributed to π-bonding interactions between the pyridyl π or π* orbitals and appropriate metal d orbitals and also to a lower ring strain for the formation of chelate rings involving pyridine-containing ligands.[33] However, this behaviour was not observed for the complexes of the parent L^3, nor for those of other cyclic amines containing pyridine in the ring with larger cavity size.[11] (5) When stabilities of the metal L^1 complexes of are compared with those of the parent L^3 (ref. 11) the values for the former are always higher, which is an indication of the co-ordination of at least one acetate group. The complexes of Cu^{2+} and Ni^{2+} have an exceptional behaviour.

It is possible to infer from the comments above that L^1 is an interesting compound for medical applications, as a contrast-enhancing agent in MRI using the manganese complex (see Fig. 6) or in nuclear medicine using ^{67}Ga or ^{111}In radioisotopes for radioimmuno-scintigraphy or ^{68}Ga for positron emission tomography.[9] At physiological pH, the competition between protons and Ga^{3+} or In^{3+} can be appreciated for L^1 and dota from the pM values, Table 5.[34] Additionally these trivalent metal complexes are neutral, the osmolarity of solutions injected intravenously is lower and therefore more suited for diffusion into tissues,[9,35] if no important toxic problems occur.

Structural data

We could not obtain crystals of the complexes appropriate for X-ray diffraction analysis, but magnetic moment measurements and spectroscopic studies in solution provided some insight into the arrangement of ligand donor atoms around the metal ion.

The electronic spectrum of the cobalt complex, yielding near-infrared and visible absorption, together with a low value of the magnetic moment, points out to a five-co-ordinate symmetry of a high-spin species. Probably in our spectrum a low-intensity band in the near-IR region (at about 1500–2000 nm) is missing, because we could not record the spectra in this range.[36–41] It is difficult by electronic spectra to distinguish between a high-spin square-pyramidal and a trigonal-bipyramidal geometry for cobalt(II) complexes especially if there is considerable distortion from an idealised structure, but in general the former leads to lower intensities (often < 100 dm^3 mol^{-1} cm^{-1}).[39,40,42–44] In our case, the similarity of the spectrum with that of a tetragonally distorted six-co-ordinate species, and the low intensities of the bands, points out to a square-pyramidal geometry for the Co^{2+}. The intense band at 295.7 nm is probably a charge-transfer band.

The electronic spectrum of the nickel complex exhibits three important and well defined bands at 954.3, 547.7 and 335.7 nm with two shoulders at 1166 and 628.2 nm, characteristic of five-co-ordinate high-spin derivatives.[40,42,43,45] The magnetic moment also falls in the range normally observed for high-spin five-co-ordinate nickel(II) species.[40,44] The band at 290.0 nm is probably also a charge-transfer band. The spectrum shows an intense band in the near-IR region and the exact number of bands expected for the allowed transitions in D_{3h} symmetry,[45] therefore a trigonal-bipyramidal arrangement around the Ni^{2+} is probable. Indeed, in C_{4v} symmetry low-energy transitions are generally found in the near-IR region.

However, in the absence of X-ray diffraction analysis the actual stereochemical arrangement of five-co-ordinate Co^{2+} or Ni^{2+} is not certain. The non-equivalence of the donor atoms of this ligand also contributes to the difficulty of assignment of a strictly trigonal-bipyramidal or a square-pyramidal geometry, and probably an intermediate structure between them actually occurs.

It is well known that electronic spectra of copper complexes are not especially good indicators of geometry,[46] however some comparisons are possible with similar complexes. In Table 6 are compiled the hyperfine coupling constants and g values for $[CuL^1]^-$ and also for other complexes taken from the literature. The EPR spectrum of $[CuL^1]^-$ is a result of a mixture of two isomers. One, **X**, with $g_z > (g_x + g_y)/2$, which is typical of rhombic symmetry of copper(II) where distortion takes the form of elongation of axial bonds, and a $d_{x^2-y^2}$ ground state is present, and consistent with elongated rhombic-octahedral or distorted square-based pyramidal stereochemistries.[46,47,51] The other isomer, **Y**, shows a very unusual spectrum with a g value only slightly greater than 2.00, consistent with a d_{z^2} ground state typical of a trigonal-bipyramidal stereochemistry, an axially compressed square pyramid, or a tetragonal structure involving compression of axial bonds.[48,52] The values of g and A (copper hyperfine coupling tensor) are similar to those found for the isomer (2*R*,5*S*,8*R*,11*S*)-1,4,7,10-tetrabenzyl-2,5,8,11-tetraethyl-1,4,7,10-tetraazacyclododecane, also a derivative of a 12-membered tetraazamacrocycle, for which an axially compressed square-pyramidal geometry with Cu^{2+} was reported (see Table 6).[48] In our case the best simulation of the spectrum was found for the ratio 1.6:1 (**X**:**Y**).

The electronic properties of isomer **X** can be compared with those of other similar copper complexes compiled in Table 6 and are explained by the usual factors taken from the equations of the EPR parameters derived from ligand-field theory.[53–55] The addition of a fifth ligand to a square-planar

Table 6 The EPR data for the copper complexes of L^1 and other similar complexes

Complex	λ/nm (ε/dm³ mol⁻¹ cm⁻¹)	EPR g_x	g_y	g_z	10^4A_x/cm⁻¹	10^4A_y/cm⁻¹	10^4A_z/cm⁻¹	Geometry[a]	Ref.
$[CuL^1]^-$	1260 (18.7),	2.039	2.093	2.269	4.1	3.9	103.9	**X**	This work
	720 (104.6)	2.272	2.161	2.007	138.3	6.9	10.2	**Y**	This work
$[CuL^3]^{2+}$	695 (161)	2.033	2.084	2.210	26.6	38.9	161.0	*SPY*	11
$[CuL^5]^{2+}$[b]	599 (220)	2.057		2.198	24.1		184.2	*SPY*	49
$[CuL^5][NO_3]_2$	590 (257)	2.089		2.172	32		175	*SPY*	47
$[CuL^6][NO_3]_2$[c]	614 (500)	2.038		2.212	31		170	*SPY*	47
$[CuL^A]^{2+}$[d]	694 (570)	2.056		2.218	13		175	*SPY*	48
$[CuL^B]^{2+}$	730 (570)	2.048	2.076	2.223	24	25	165	*SPY*	48
$[CuL^C]^{2+}$	775 (545)	2.047	2.092	2.230	14	24	161	*SPY*	48
$[CuL^D]^{2+}$	1149 (221),	2.232	2.139	2.014	127	64	44	*e*	48
	883 (285)								
$[Cu(dota)]^{2-}$	734 (100)	2.062		2.300	—	—	150.3	*OC*	50
$[CuL^7]^{2+}$[f]	513 (100)	2.049		2.186	38.7		205.0	*SP*	49
$[Cu(teta)]^{2-}$	646 (70)	2.050		2.249	—	—	168.0	*OC*	50

[a] *SPY* = Square pyramid, *OC* = octahedron, *SP* = Square Planar. [b] L^5 = 1,4,7,10-Tetraazacyclododecane. [c] L^6 = 1,4,7,10-Tetrabenzyl-1,4,7,10-tetraazacyclododecane. [d] L^A = (2*R*,5*R*,8*R*,11*R*) or (2*S*,5*S*,8*S*,11*S*) isomer of 1,4,7,10-tetrabenzyl-2,5,8,11-tetraethyl-1,4,7,10-tetraazacyclododecane; L^B = the (2*R*,5*R*,8*S*,11*S*) isomer; L^C = the (2*S*,5*R*,8*R*,11*R*) or (2*R*,5*S*,8*S*,11*S*) isomer and L^D = the (2*R*,5*S*,8*R*,11*S*) isomer. [e] Axially compressed *SPY*. [f] L^7 = 1,4,8,11-Tetraazacyclotetradecane (cyclam).

arrangement has the effect of decreasing A_z while increasing g_z[56,57] with a simultaneous red shift in the electronic spectrum. In general, we can see that the energies of the visible band of the complexes decrease in the same order as the $|A_z|$ values, but in the reverse sequence of the g_z values. This sequence in principle parallels the extent of distortion from C_{4v} square-pyramidal geometry. Comparing the complex of the parent L^3 with that of L^1 (isomer **X**) there is an increase in g_z, a decrease in A_z and a red shift of the electronic spectrum. As the structure of the copper L^3 complex was already considered square pyramidal, it is possible to infer that the structure of $[CuL^1]^-$ will be a more distorted square pyramid. This **X** isomer has the lowest value of A_z in Table 6, one of the highest values of g_z, and the band in its electronic spectrum is more displaced to lower energies, which means a very distorted square-pyramidal structure. The other isomer would have either an axially compressed square-pyramidal or a trigonal-bipyramidal structure. However, it was suggested that square-pyramidal copper(II) complexes have an absorption band in the region 550–670 nm, while trigonal-bipyramidal complexes absorb near 800–850 nm (d_{xy}, $d_{x^2-y^2} \longrightarrow d_{z^2}$), with a higher-energy shoulder (spin-forbidden d_{xz}, $d_{yz} \longrightarrow d_{z^2}$).[47,58,59] The fact that in our complex the transition is observed at higher energy points to an axially compressed square-pyramidal geometry.

The electronic spectrum of the iron(III) complex, as expected for a d^5 configuration, gives no information because the tail of the intense charge-transfer absorptions overlap the weak forbidden bands of the visible region, producing the yellow colour. The bands at 286.8 and 257.9 nm are assigned to metal-to-ligand charge-transfer transitions owing to the relatively high absorption coefficients. The EPR spectra of this complex at 4.6, 100.0 and 200.0 K are characteristic of high-spin iron(III) in a rhombically distorted electronic environment. The EPR spectrum of high-spin Fe^{3+} can be described by the spin Hamiltonian (3) where $S = \frac{5}{2}$, $g_0 = 2.0$ and

$$H = g_0\beta\vec{H}\cdot\vec{S} + D\{S_z^2 - \tfrac{1}{3}S(S+1) + [E/D\,(S_x^2 - S_y^2)]\} \quad (3)$$

D and *E* are the axial and rhombic zero-field splitting parameters, respectively. The zero-field-splitting term (*D*, *E*) partly removes the degeneracy of the spin sextet and three Kramer's doublets result.[60,61] If the separation of the doublets is large compared to βH, and if the electron spin relaxation is sufficiently slow, each doublet is expected to give rise to its own resonance, which can be described in terms of an effective $S = \frac{1}{2}$ spectrum with three *g* values, not all observed.[60,62] The resulting nine *g* values depend on the parameter *E*/*D*. The *g* values obtained for the $[FeL^1]$ complex can be well reproduced by the rhombicity parameter $E/D = 0.142$, which corresponds to an intermediate rhombicity.[61] The *D* value would be low, or even close to zero, as the spectra at 4.6, 100.0 and 200.0 K do not show differences in the relative intensity of the peaks. For the *E*/*D* value found, it is possible to obtain *g* values of 8.589, 2.847 and 1.482 for the ground doublet ($S_z = \frac{1}{2}$), 5.435, 2.713 and 3.009 for the middle one ($S_z = \frac{3}{2}$), and 9.953, 0.125 and 0.144 for the upper ($S_z = \frac{5}{2}$) doublet. Indeed, Fig. 4 shows the resonance at $g \approx 8.6$ corresponding to the ground doublet, that at $g \approx 5.4$ of the middle one, that at $g \approx 9.9$ of the upper doublet and the broad resonance at $g \approx 3$ which would correspond to the resonances at 2.847 of the ground doublet and 2.713 and 3.009 of the middle one. The additional signal observed at $g = 4.27$ can be attributed to the other isomer, corresponding to the middle $|S_z = \frac{3}{2}\rangle$ doublet of another high-spin iron(III) ion with $E/D \approx \frac{1}{3}$. This EPR spectrum is similar to that observed for some non-haem iron proteins like desulfoferrodoxin from *Desulfovibrio desulfuricans*[63,64] or an iron-containing blue protein, neelaredoxin, isolated from the sulfate-reducing bacterium *Desulfovibrio gigas*.[65] It has been proposed that one of the centres of desulfoferrodoxin is similar to the iron centres of neelaredoxin, and that the iron co-ordination involves in both cases nitrogen and/or oxygen ligands,[63–65] probably in a five-co-ordinated geometry, as well as in other non-haem iron proteins containing mononuclear centres.[66,67] So, the macrocycle studied in the present work should be a good model for the study of the metal centre of these proteins.

Conclusion

In spite of forming less stable complexes than those of dota, L^1 has a lower overall basicity making it a better candidate for specific medical applications, such as a contrast-enhancing agent in magnetic resonance imaging using the manganese(II) complex or in nuclear medicine using ^{67}Ga, ^{68}Ga or ^{111}In. Complexes of L^1 with Ga^{3+} or In^{3+} have low osmolarity as they are neutral, while dota forms charged complexes. Also, L^1 forms complexes with Fe^{3+} which have EPR spectra similar to those of some proteins and should be a good model for the study of their metal centres. A very curious fact related with L^1 is that its complexes with the first-row transition-metal ions do not obey the Irving–Williams trend, the stability of the nickel complex being lower than that of the cobalt one, and the copper complex is less stable than that of Ni^{2+}. The copper complex has the lowest stability of this series, a very peculiar situation. However,

other cases exist where the cobalt(II) complexes are more stable than those of Ni^{2+}: for dota (although the difference in stabilities of both complexes is very small),[2,3] for L [4] (ref. 24) and also for 1,4,10-trioxa-7,13-diazacyclopentadecane-7,13-diacetate,[68] only to mention cases involving *N*-acetate derivatives of azamacrocyclic ligands (other examples are in the references of the last articles mentioned). This situation may occur with five-co-ordinate complexes, either square pyramidal or trigonal bipyramidal. In this geometry the Co^{2+} (d^7) will be more favoured in terms of crystal-field stabilisation energy (CFSE) than Ni^{2+} (d^8), and the increase in stability expected from the increase in atomic number (which usually occurs for octahedral symmetries) may not compensate the loss of CFSE.[68,69] The low value for the copper(II) complex is more difficult to explain, as it is known that this metal ion is more stable when five-co-ordinate.[69] Probably, to form this geometry around the metal ion all the nitrogen donor atoms of the ligand do not co-ordinate.

Acknowledgements

The authors acknowledge financial support from Junta Nacional de Investigação Científica e Tecnológica (Project no. PBIC/P/QUI/1643/93). One of us (A. Z.) thanks Fundação Oriente for funding.

References

1 H. Stetter, W. Frank and R. Mertens, *Tetrahedron*, 1981, **37**, 767.
2 R. Delgado and J. J. R. Fraústo da Silva, *Talanta*, 1982, **29**, 815.
3 S. Chaves, R. Delgado and J. J. R. Fraústo da Silva, *Talanta*, 1992, **39**, 249.
4 M. T. S. Amorim, R. Delgado and J. J. R. Fraústo da Silva, *Polyhedron*, 1992, **11**, 1891.
5 M. T. Beck and I. Nagypál, *Chemistry of Complex Equilibria*, Ellis Horwood, Chichester, 1990, pp. 348–350.
6 M. F. Loncin, J. F. Desreux and E. Merciny, *Inorg. Chem*., 1986, **25**, 2646.
7 W. P. Cacheris, S. K. Nickle and A. D. Sherry, *Inorg. Chem.*, 1987, **26**, 958.
8 X. Wang, T. Jin, V. Comblin, A. Lopez-Mut, E. Merciny and J. F. Desreux, *Inorg. Chem.*, 1992, **31**, 1095.
9 V. Alexander, *Chem. Rev.*, 1995, **95**, 273.
10 S. P. Kasprzyk and R. G. Wilkins, *Inorg. Chem*., 1982, **21**, 3349.
11 J. Costa and R. Delgado, *Inorg. Chem.*, 1993, **32**, 5257.
12 W. D. Kim, D. C. Hrncir, G. E. Kiefer and A. D. Sherry, *Inorg. Chem.*, 1995, **34**, 2225.
13 W. D. Kim, G. E. Kiefer, F. Maton, K. McMillan, R. N. Muller and A. D. Sherry, *Inorg. Chem.*, 1995, **34**, 2233.
14 D. D. Perrin and W. L. F. Armarego, *Purification of Laboratory Chemicals*, 3rd edn., Pergamon, Oxford, 1988.
15 C. F. G. C. Geraldes, R. Delgado, A. M. Urbano, J. Costa, F. Jasanada and F. Nepveu, *J. Chem. Soc., Dalton Trans.*, 1995, 327.
16 L. Pehrsson, F. Ingman and A. Johansson, *Talanta*, 1976, **23**, 769.
17 E. Bottari and G. Anderegg, *Helv. Chim. Acta*, 1967, **50**, 2349.
18 P. Gans, A. Sabatini and A. Vacca, *J. Chem. Soc., Dalton Trans.*, 1985, 1195.
19 A. E. Martell and R. J. Motekaitis, *Determination and Use of Stability Constants*, 2nd edn., VCH, New York, 1992.
20 D. J. Leggett and W. A. E. McBryde, *Anal. Chem.*, 1975, **47**, 1065; D. J. Leggett, *Anal. Chem.*, 1978, **50**, 718.
21 R. Delgado, Y. Sun, R. J. Motekaitis and A. E. Martell, *Inorg. Chem*., 1993, **32**, 3320.
22 D. F. Evans, *J. Chem. Soc.*, 1959, 2003.
23 F. Neese, Diploma Thesis, University of Konstanz, June 1993.
24 (*a*) M. T. S. Amorim, R. Delgado, J. J. R. Fraústo da Silva, M. C. T. A. Vaz and M. F. Vilhena, *Talanta*, 1988, **35**, 741; (*b*) M. T. S. Amorim, Ph.D. Thesis, Lisbon, 1993.
25 E. T. Clarke and A. E. Martell, *Inorg. Chim. Acta*, 1991, **190**, 37.
26 (*a*) R. M. Smith, A. E. Martell and R. J. Motekaitis, *Nist Critical Stability Constants of Metal Complexes Database*, U.S. Department of Commerce, Gaithersburg, 1993; (*b*) L. D. Pettit and H. K. J. Powell, *IUPAC Stability Constants Database*, Academic Software, Timble, 1993.
27 J. R. Ascenso, R. Delgado and J. J. R. Fraústo da Silva, *J. Chem. Soc., Perkin Trans. 2*, 1985, 781.
28 M. T. S. Amorim, J. R. Ascenso, R. Delgado and J. J. R. Fraústo da Silva, *J. Chem. Soc., Dalton Trans.*, 1990, 3449.
29 A. Riesen, M. Zehnder and T. A. Kaden, *J. Chem. Soc., Chem. Commun.*, 1985, 1336.
30 A. Riesen, M. Zehnder and T. A. Kaden, *Helv. Chim. Acta*, 1986, **69**, 2067.
31 A. Riesen, M. Zehnder and T. A. Kaden, *Helv. Chim. Acta*, 1986, **69**, 2074.
32 V. Felix, M. J. Calhorda, J. Costa, R. Delgado, C. Brito, M. T. Duarte, T. Arcos and M. G. B. Drew, *J. Chem. Soc., Dalton Trans.*, 1996, 4543.
33 J. H. Timmons, A. E. Martell, W. R. Harris and I. Murase, *Inorg. Chem*., 1982, **21**, 1525.
34 S. M. Madsen, C. J. Bannochie, A. E. Martell, C. J. Mathias and M. J. Welch, *J. Nucl. Med.*, 1990, **31**, 1662.
35 K. Kumar and M. F. Tweedle, *Pure Appl. Chem.*, 1993, **65**, 515.
36 L. Sacconi and G. P. Speroni, *Inorg. Chem*., 1968, **7**, 295.
37 I. Bertini and C. Luchinat, *Adv. Inorg. Biochem*., 1984, **6**, 71.
38 C. M. Sarther and E. L. Blinn, *Inorg. Chem*., 1976, **15**, 3083.
39 Y.-Y. Chen, D. E. Chu, B. D. McKinney, L. J. Willis and S. C. Cummings, *Inorg. Chem*., 1981, **20**, 1885.
40 A. B. P. Lever, *Inorganic Electronic Spectroscopy*, 2nd edn., Elsevier, Amsterdam, 1984.
41 S. Bürki and T. A. Kaden, *J. Chem. Soc., Dalton Trans.*, 1991, 805.
42 M. Ciampolini and N. Nardi, *Inorg. Chem*., 1966, **5**, 41; 1967, **6**, 445.
43 L. Sacconi, R. Morassi and S. Midollini, *J. Chem. Soc. A*, 1968, 1510.
44 R. Smierciak, J. Passariello and E. L. Blinn, *Inorg. Chem*., 1977, **16**, 2646.
45 M. Ciampolini, *Inorg. Chem.*, 1966, **5**, 35.
46 B. J. Hathaway, *Coord. Chem. Rev.*, 1983, **52**, 87.
47 M. C. Styka, R. C. Smierciak, E. L. Blinn, R. E. DeSimone and J. V. Passariello, *Inorg. Chem*., 1978, **17**, 82.
48 N. Azuma, Y. Kohno, F. Nemoto, Y. Kajikawa, K. Ishizu, T. Takakuwa, S. Tsuboyama, K. Tsuboyama, K. Kobayashi and T. Sakurai, *Inorg. Chim. Acta*, 1994, **215**, 109.
49 K. Miyoshi, H. Tanaka, E. Kimura, S. Tsuboyama, S. Murata, H. Shimizu and H. Ishizu, *Inorg. Chim. Acta*, 1983, **78**, 23.
50 R. Delgado, J. J. R. Fraústo da Silva and M. C. T. A. Vaz, *Talanta*, 1986, **33**, 285.
51 T. Vänngard, in *Biological Application of Electron Spin Resonance*, ed. by H. M. Swartz, J. R. Bolton, D. C. Borg, Wiley-Interscience, 1972.
52 B. J. Hathaway and A. A. G. Tomlinson, *Coord. Chem. Rev.*, 1970, **5**, 1.
53 H. R. Gersmann and J. D. Swalen, *J. Chem. Phys.*, 1962, **36**, 3221.
54 H. Yokoi, M. Sai, T. Isobe and S. Ohsawa, *Bull. Chem. Soc. Jpn.*, 1972, **45**, 2189.
55 P. W. Lau and W. C. Lin, *J. Inorg. Nucl. Chem*., 1975, **37**, 2389.
56 A. W. Addison, M. Carpenter, L. K.-M. Lau and M. Wicholas, *Inorg. Chem.*, 1978, **17**, 1545.
57 M. J. Maroney and N. J. Rose, *Inorg. Chem*., 1984, **23**, 2252.
58 B. J. Hathaway, in *Comprehensive Coordination Chemistry*, eds. G. Wilkinson, R. D. Guillard and J. A. McCleverty, Pergamon, Oxford, 1987, vol. 5, p. 533.
59 G. A. McLachlan, G. D. Fallon, R. L. Martin and L. Spiccia, *Inorg. Chem*., 1995, **34**, 254.
60 W. R. Hagen, *Adv. Inorg. Chem.*, 1992, **38**, 165.
61 G. Palmer, in *The Porphyrins*, ed. D. Dolphin, Academic Press, New York, 1979, vol. 4, pp. 313–353.
62 W. Whittaker, J. D. Lipscomb, T. A. Kent and E. Munck, *J. Biol. Chem.*, 1984, **259**, 4466.
63 I. Moura, P. Tavares, J. J. G. Moura, N. Ravi, B. H. Huynh, M.-Y. Liu and J. LeGall, *J. Biol. Chem.*, 1990, **265**, 21596.
64 P. Tavares, N. Ravi, J. J. G. Moura, J. LeGall, Y.-H. Huang, B. R. Crouse, M. K. Johnson, B. H. Huynh and I. Moura, *J. Biol. Chem.*, 1994, **269**, 10504.
65 L. Chen, P. Sharma, J. LeGall, A. M. Mariano, M. Teixeira and A. V. Xavier, *Eur. J. Biochem*., 1994, **226**, 613.
66 S. Navaratnam, M. C. Feiters, M. Al-Hakim, J. C. Allen, G. A. Veldink and J. F. G. Vliegenthart, *Biochim. Biophys. Acta*, 1988, **956**, 70.
67 J. C. Boyington, B. J. Gaffney and L. M. Amzel, *Science*, 1993, **260**, 1482.
68 R. Delgado, J. J. R. Fraústo da Silva, M. C. T. A. Vaz, P. Paoletti and M. Micheloni, *J. Chem. Soc., Dalton Trans.*, 1989, 133.
69 C. Furlani, *Coord. Chem. Rev.*, 1968, **3**, 141.

Received 2*nd April* 1996*; Paper* 6/02311H